International Journal of Technology (2015) 7: 1191-1197
ISSN 2086-9614

CORROSION RESISTANCE ENHANCEMENT OF AN ANODIC LAYER ON AN ALUMINUM MATRIX COMPOSITE BY CERIUM SEALING

Vika Rizkia[1,2*], Badrul Munir[1], Johny Wahyuadi Soedarsono[1], Bambang Suharno[1]

[1] *Department of Metallurgy and Materials Engineering, Faculty of Engineering, Universitas Indonesia, Kampus Baru UI Depok, Depok 16424, Indonesia*
[2]*Departement of Mechanical Engineering, State Polythechnic of Jakarta*
Jl. Prof. Dr. G.A Siwabessy, Kampus Baru UI Depok, Depok 16425, Indonesia

(Received: June 2015 / Revised: September 2015 / Accepted: September 2015)

ABSTRACT

The anodizing process was conducted in an Al7xxx aluminum alloy with silicon carbide which yielded a non-uniform thickness of anodic film with cavities, micro-pores and micro-cracks within it. This phenomenon occurred due to the presence of Silicon Carbide (SiC) particles within the Aluminum Matrix Composite (AMC), which impedes the initiation and growth of the protective anodic alumina oxide layer. Therefore, cerium sealing has been considered as the cheapest and simplest post treatment to remedy the poor anodic alumina oxide film in order to further enhance the corrosion resistance in aggressive circumstances. This paper examined the protection effect of an integrated layer which was composed of an anodized oxide layer and cerium deposits on an Al7075/SiC composite. Electrochemical Impedance Spectroscopy (EIS) was used to examine the corrosion protection effect and the corrosion behavior of an integrated layer in 3.5% sodium chloride (NaCl) solution at room temperature. In this study, anodizing of Al7075/SiC was carried out in a sulfuric acid H2SO4 solution at current density values of 15, 20, and 25 mA/cm^2, respectively at room temperature, 0^{o}C and -25^{o}C for 30 minutes. Subsequently, cerium sealing was conducted in a cerium choloride plus hydrogen peroxide (CeCl3.6H2O + H2O2) solution at room temperature and pH 9 for 30 minutes. The best protection effect was found for Al7075/SiC, anodized at 0^{o}C. Field Emission-Scanning Electron Microscope (FE-SEM) examination confirmed that the enhancement of corrosion resistance was due to the cerium deposit formed on the entire surface of the oxide anodized layer.

Keywords: Aluminum Matrix Composite; Anodizing; Cerium sealing; Corrosion

1. INTRODUCTION

Aluminum Matrix Composite (AMC) becomes a promising material for the automotive and aerospace industries due to its superior combination of properties compared to an unreinforced aluminum alloy. AMC offers a high strength to weight ratio, a low thermal expansion coefficient and relatively good wear resistance (Yu & Lee, 2000). The current and AMC potential applications are piston rings, combustion piston bowls, cylinder liners, and connecting rods in the automotive sector, aircraft structural framework, and aircraft engines in the aerospace sector (Amirkhanlou & Niroumand, 2011; Bobic et al., 2010). However, these materials are generally susceptible to pitting and galvanic corrosion due to galvanic reaction

* Corresponding author's email: vee_mt03@yahoo.com, Tel. +62-21-786 3510, Fax. +62-21-787 2350
Permalink/DOI: http://dx.doi.org/10.14716/ijtech.v6i7.1260

between the aluminum matrix and the reinforcement, as well as the microstructure formation at the matrix/reinforcement interface (Bienia et al., 2003; Amirkhanlou & Niroumand, 2011; Bobic et al., 2010. Therefore, a surface coating or an AMC modification process is a necessity in order to improve corrosion resistance.

Anodizing has been considered as the most suitable and potential surface modification method for enhancing AMC corrosion resistance. This process produces a porous anodic alumina oxide layer, which has the characteristics of high corrosion resistance and high hardness value (Hou & Chung, 1997; Sun et al., 2009). Various studies of the anodizing process on aluminum matrix composite material (AMC) generate the anodic alumina oxide layer formed on the surface of an anodized AMC with much higher corrosion and wear resistance than that of an unanodized AMC (Derman & Ahmad, 2007; He et al., 2011a; He et al., 2008; Shahid, 1997).

Unfortunately, the oxide layer obtained on the AMC surface has an uneven thickness and many cavities occur due to the disturbing effect of the reinforcement particles on the anodic oxide layer growth (He et al., 2011b; He et al., 2008; Rizkia et al., 2014). Therefore in aggressive circumstances, a single anodic film protection is not enough. Cerium sealing is considered as the cheapest and simplest post-treatment to seal the surface defects of the anodic film in order to further enhance corrosion resistance. Many researchers have found that the cerium sealing layer is composed of spherical cerium oxide/hydroxide deposits, which not only seal the porous structures of anodized AMC, but also cover most of the defects. Moreover, integrated protection processes performed on the AMC produced much higher corrosion resistance as well as that of pure aluminum (Sun et al., 2009; Sun et al., 2008; Yu et al., 2002).

2. EXPERIMENTAL

The specimens were Al7xxx alloys containing 15 vol% of SiC particles with the dimension of 10×10 mm^2. Prior to anodizing, the specimens were prepared according to standard metallographic preparation procedures, which were sanded successively with #100 to #1000 abrasive papers, rinsed with acetone then immersed in a HNO_3 solution at room temperature for 30 seconds. In order to produce an integrated layer, specimens were anodized at constant current densities of 15, 20, and 25 mA/cm^2 respectively applied by DC Power Supply in 16% sulfuric acid H_2SO_4 solution at room, 0 ± 0.5^oC, and $-25\ \pm0.5^oC$ for 30 minutes. A carbon bar was used as the cathode. Subsequently, an anodized composite was immersed in $CeCl_3+H_2O_2$ solution at room temperature with pH 9 for 30 minutes. The corrosion protection effect and corrosion behavior of the integrated layer in 3.5% NaCl solution were examined by Electrochemical Impedance Spectroscopy (EIS). A Field Emission–Scanning Electron Microscope (FE-SEM FEI Inspect F50) was used for examination of the SEM integrated coating morphology.

3. RESULTS AND DISCUSSION

In this research, EIS studies were conducted to evaluate the corrosion protection effect of an integrated layer of aluminum anodic oxide and cerium layer on Al7075/SiC composite with different anodizing temperatures and current densities. The different shapes of *nyquist* plots as seen in Figure 1 indicates that different corrosion mechanisms occurred in different anodizing temperatures and current densities in this research.

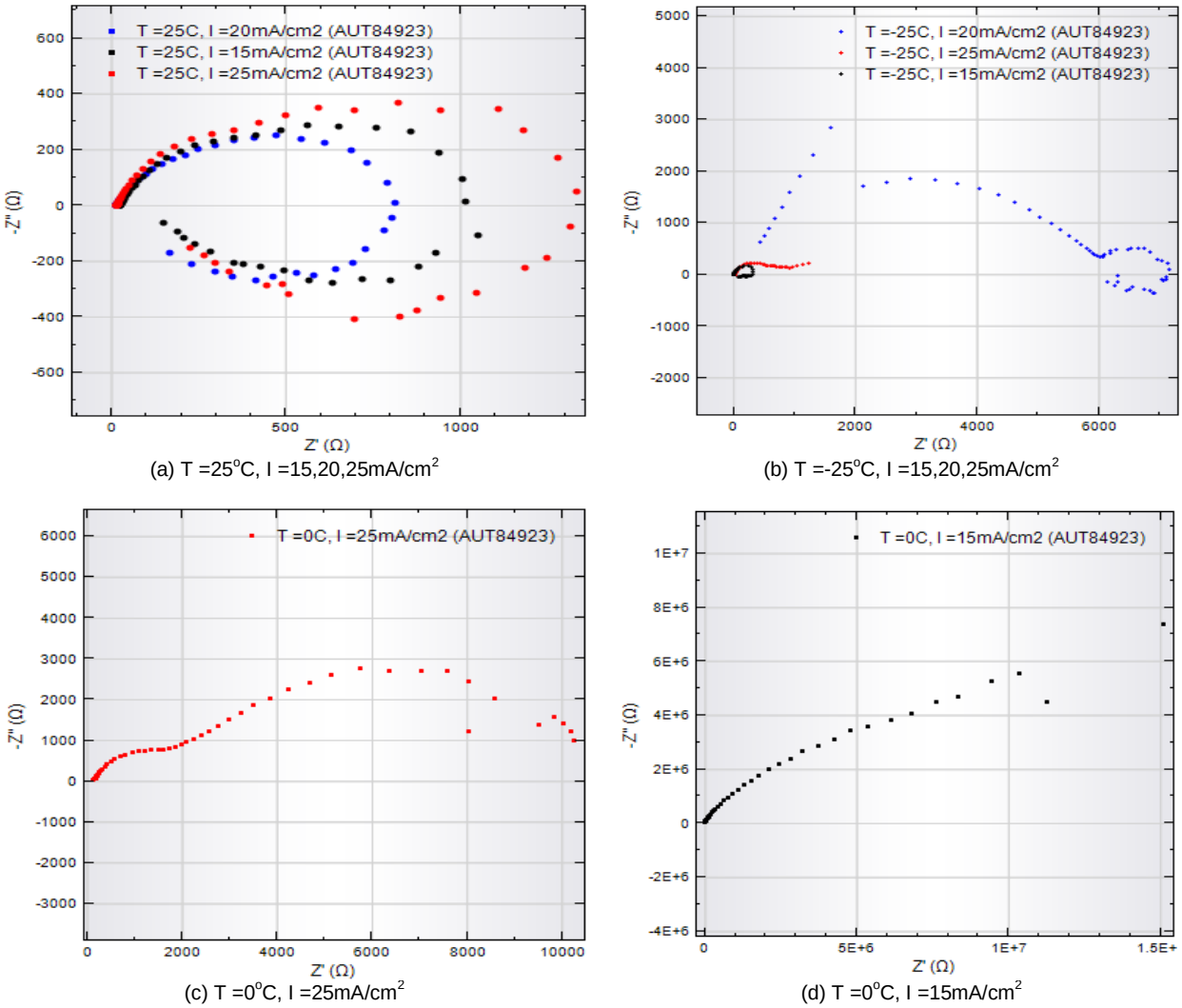

(a) T =25°C, I =15,20,25mA/cm^2

(b) T =-25°C, I =15,20,25mA/cm^2

(c) T =0°C, I =25mA/cm^2

(d) T =0°C, I =15mA/cm^2

Figure 1 Nyquist plot of anodized Al7075/SiC after cerium sealing process

As we have seen in Figure 1, by analyzing the nyquist plots, it can be deduced that the anodizing process at room temperature for all of the studied potential conditions exhibited one capacitive semicircle in the high frequency region and one inductive loop in the low frequency region. A capacitive semicircle in the high-frequency region, related to the characteristics of Electrical Double Layer (EDL), was formed at the interface between the adsorption layer on the metal surface and the electrolyte (Katkar et al., 2011). Furthermore, some researchers reported that the appearance of the inductive loop at a low frequency range indicated that the alloy surface is partly or totally active (Hasannejad et al., 2011; Katkar et al., 2011; Zhang et al., 2009). In this research, inductive phenomenon could be associated with a loose or damaged anodic alumina oxide layer on the Al7075/SiC surface in a chloride solution. This phenomenon leads to the adsorption of chloride ions into the composite substrate, since no cerium layer was formed in this condition as reported in the FE-SEM analysis by Munir et al. (2014). Moreover, a single capacitive curve as seen in Figure 1a indicated that only one anodic alumina oxide layer formed on Al7075/SiC surface in the aforementioned condition. The similar curve can also be noted from the anodizing process at a temperature of -25°C and with a current density of 15mA/cm^2.

In the anodizing process at temperature of 0°C, the nyquist plot is characterized with one capacitive semicircle in the high frequency region and additional capacitive semicircle at low frequency region. It may be correlated to the formation of integrated layer composed of anodic alumina oxide layer and cerium deposits as reported in previous work (Munir et al., 2014). The high frequency of nyquist plot depicts the resistance Rce and capacitance Cce of the cerium sealing layer, while the low frequency depicts the resistance Ro and capacitance Co of an anodic alumina oxide layer (Sun et al., 2011). Yet, capacitance Cce and Co have some distinctions from a pure capacitance element C. Those capacitances are substituted by constant phase elements of Qce and Qo, respectively (Hui et al., 2004). Therefore the electrochemical equivalent circuit for EIS of an anodized Al7075/SiC composite at 0°C anodizing condition is shown in Figure 2, where, Rsol is the electrolyte solution resistance.

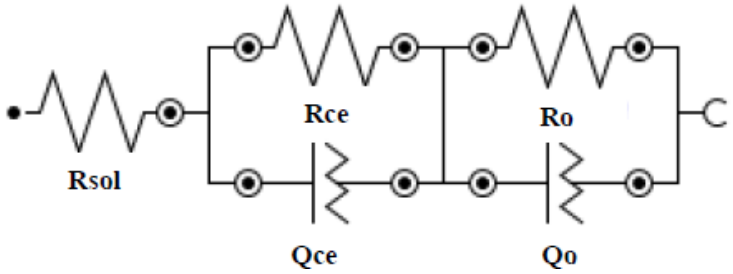

Figure 2 Equivalent electrical circuit used to interpret the experimental EIS data of cerium treated on as anodized Al7075/SiC composite at 0°C

At an anodizing temperature of -25°C at 25 mA/cm^2, the nyquist plot shows a capacitive semicircle in the high-frequency region and linear curve in the low frequency region which exhibits the characteristics of diffuse control. In this condition, the corrosion medium has penetrated through the alumina anodic oxide layer and immigrated into the substrate which leads to the corrosion phenomenon on the Al7075/SiC composite. The electrochemical equivalent circuit shown in Figure 3 is suitable to simulate this condition, where Rsol is solution resistance; Ra and Qa are resistance and constant phase elements of broken anodic alumina oxide layer, respectively. Then, Rs and Qs are the electrochemical transaction resistance and constant phase elements of the aluminum matrix, respectively. Then, W is the transmission line parameter or the Warberg impedance, indicative of the diffusion rate reacting to the species (Sun et al., 2011).

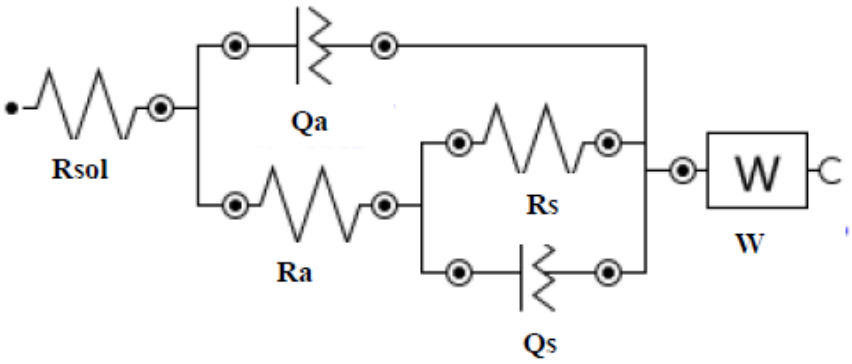

Figure 3 Equivalent electrical circuit used to fit the corrosion behavior of cerium treatment on an anodized Al7075/SiC composite at -25°C and 25 mA/cm^2

For the anodizing temperature of -25^{o}C at 20 mA/cm^{2}, the nyquist plot shows two capacitive semicircles, which are related to the characteristics of the electrical double layer (EDL) which formed at the interface between the adsorption layer on composite surface and the electrolyte. Moreover, an additional inductive loop appeared after two of the aforementioned capacitive semicircles. This phenomenon may be correlated with the formation of two anodic alumina oxide layers composed of a barrier oxide layer at the inner region and worm-like shaped porous oxide at the outer region (Munir et al., 2014) , and it continued on with the damage of those oxide layers. The high frequency range of the nyquist plot represents the resistance Rp and the constant phase element Qp of the broken worm-like shaped porous oxide. While in the low frequency range of the nyquist plot, it represents the resistance Rb and the constant phase element Qb of the broken barrier anodic oxide. Moreover, an inductive semicircle in the low frequency range represents the breakdown of anodic alumina oxide layers on the Al7075/SiC surface in a chloride solution. It indicates that the corrosion medium has been penetrated with the worm-like shaped porous oxide layer and a barrier layer, which leads to the corrosion reaction of Al7075/SiC controlled by the charge-transfer. Therefore, the equivalent circuit in this case is shown in Figure 4, where Rt is the resistance of charge-transfer and Qdl is a constant phase element of the double layer.

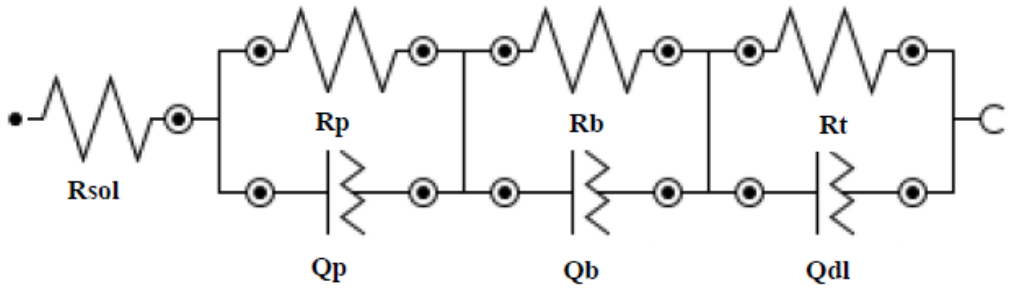

Figure 4 Equivalent electrical circuit used to fit the corrosion behavior of cerium treated as an anodized Al7075/SiC composite at -25^{o}C and 20 mA/cm^{2}

Furthermore, according to Figure 1 the largest curve and highest impedance (Z) value is attained from the samples which were cerium treated after the anodizing process at the temperature of 0^{o}C. In addition, the EIS plots of that condition exhibit no corrosion medium had penetrated into the composite substrate, which leads a non-corrosion reaction on the Al7075/SiC composite. This condition occurred due to the fact that the cerium layer disturbs the migration of corrosive media through the pores and cavities of the anodic alumina oxide layer. Moreover, cerium deposits completely cover the pores and cavities on the anodic oxide layer which induces the blocking effect of the corrosion process on Al7075/SiC composite as seen in Figure 5b.

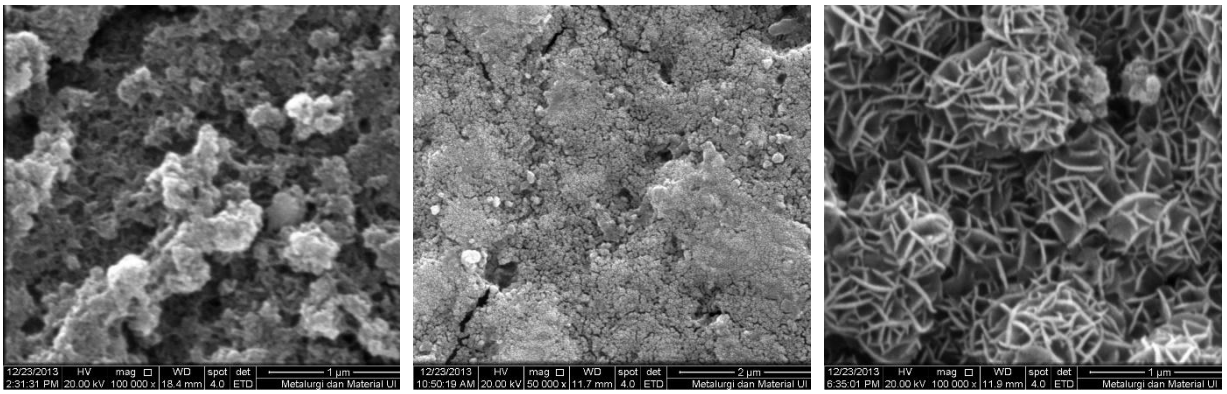

(a) (b) (c)

Figure 5 Typical FE-SEM images of anodized Al7075/SiC after the cerium sealing process at: (a) room temperature, produced only a single anodic alumina barrier layer; (b) 0^{o}C, produced integrated layer of anodic alumina oxide layer and cerium sealing layer; (c) -25^{o}C, produced two anodic alumina layers of barrier and *worm like shaped* layers

4. CONCLUSION

Corrosion protection of the Al7075/SiC composite was successfully performed on the Al7075/SiC composite by conducting cerium sealing, subsequently after anodizing process. The best protection effect was found for the Al7075/SiC, anodized at 0^{o}C. The largest curve and highest impedance value is attained from the samples treated at an anodizing temperature of 0^{o}C. Furthermore, the EIS exhibits no corrosion medium permeate onto substrate which leads to a non-corrosion reaction on the Al7075/SiC composite, due to an integrated layer composed of an anodized and a cerium layer formed on the Al7075/SiC surface.

5. ACKNOWLEDGEMENT

This study has been financed by Hibah PUPT (BOPTN) scheme, University of Indonesia.

6. REFERENCES

Amirkhanlou, S., Niroumand, B., 2011. Development of Al356/SiCp Cast Composites by Injection of SiCp Containing Composite Powders. *Materials and Design 32*, Volume 32(4), pp. 1895–1902

Bienia, J., Surowska, B., Walczak, M., 2003. The Corrosion Characteristics of Aluminium Matrix Composites Reinforced with SiC Particles. In: *Proceedings of the 12th International Scientific Conference*

Bobic, B., Mitrovic, S., Babic, M., 2010. Corrosion of Metal-matrix Composites with Aluminium Alloy Substrate. *Tribology in industry,* Volume 32(1), pp. 3–11

Derman, M.N., Ahmad, Z.A., 2007. Study of Wear on Anodized PM Aluminum Matrix Composite Reinforced with 15% Saffil TM Alumina Short Fibre. In: *Proceedings of the International Conference on Sustainable Materials*

Hasannejad, H., Shahrabi, T., Jafarian, M., Rouhaghdam, A.S., 2011. EIS Study of Nano Crystalline Ni-cerium Oxide Coating Electrodeposition Mechanism. *Journal of Alloys and Compounds,* Volume 509, pp. 1924–1930

He, C., Lou, D., Wang, J., Cai, Q., 2011a. Corrosion Protection and Formation Mechanism of Anodic Coating on SiCp/Al Metal Matrix Composite. *Thin Solid Films,* Volume 519, pp. 4759–4764

He, C., Lou, D., Wang, J., Cai, Q., 2011b. Corrosion Protection and Formation Mechanism of Anodic Coating on SiCp/Al Metal Matrix Composite. *Thin Solid Films,* Volume 519(15), pp. 4759–4764

He, C., Zhou, Q., Liu, J., Geng, X., Cai, Q., 2008. Effect of Size of Reinforcement on Thickness of Anodized Coatings on SiC/Al Matrix Composites. *Materials Letters*, Volume 62(16), pp. 2441–2443

Hou, J.Y., Chung, D.D.L., 1997. Corrosion Protection of Aluminium-matrix Aluminium Nitride and Silicon Carbide Composites by Anodization. *Journal of Material Science,* Volume 32(12), pp. 3113–3121

Hui, Z.X., Yu, Z., Mao, Z.J., 2004. Electrochemical Properties of Anodized Aluminum Films in Sodium Chloride Solution. *The Chinese Journal of Nonferrous Metals,* Volume 14(4), pp. 562–567

Katkar, V., Gunasekaran, G., Rao, A.G., Koli, P.M., 2011. Effect of the Reinforced Boron Carbide Particulate Content of AA6061 Alloy on Formation of the Passive Film in Seawater. *Corrosion Science,* Volume 53(9), pp. 2700–2712

Munir, B., Rizkia, V., Soedarsono, J.W., Suharno, B., 2014. Growth of Anodized Layer and Cerium Sealing on Al7xxx/SiC Composite. *Applied Mechanics and Materials Journal*, Volume 1119, pp. 212–217

Rizkia, V., Munir, B., Soedarsono, J.W., Suharno, B., Rustandi, A., 2014. Growth of Porous Alumina Layer and Cerium Sealing of Al7xxx/SiC Composite for Structural Lightweight Alloy Corrosion Resistant Application. *Advanced Material Research,* Volume 911, pp. 55–59

Shahid, M., 1997. Mechanism of Film Growth during Anodizing of Al-alloy-8090/SiC Metal Matrix Composite in Sulphuric Acid Electrolyte. *Journal of Materials Science*, Volume 32(14), pp. 3775–3781

Sun, H., Li, X., Chen, D., Wang, H., 2009. Enhanced Corrosion Resistance of Discontinuous Anodic Film on in situ TiB2p/A356 Composite by Cerium Electrolysis Treatment. *Journal of Materials Science,* Volume 44(3), pp. 786–793

Sun, H., Ma, N., Chen, D., Li, X., Wang, H., 2008. Fabrication and Analysis of Anti-corrosion Coatings on in-situ TiB2p Reinforced Aluminum Matrix Composite. *Surface & Coatings Technology,* Volume 203(3–4), 329–334

Sun, H., Wang, H., Meng, F., 2011. Study of Corrosion Protection of the Composite Films on A356 Aluminum Alloy. *Journal of Rare Earth,* Volume 29(10), pp. 991–996

Yu, X., Lee, W.B., 2000. The Design and Fabrication of an Alumina Reinforced Aluminum Composite Material. *Composites Part A: Applied Science and Manufacturing*, Volume 31(3), pp. 245–258

Yu, X., Yan, C., Cao, C., 2002. Study on the Rare Earth Sealing Procedure of the Porous Film of Anodized Al6061/SiCp. *Materials Chemistry and Physics,* Volume 76(3), pp. 228–235

Zhang, J., Zhang, W., Yan, C., Du, K., Wang, F., 2009. Corrosion Behaviors of Zn/Al–Mn Alloy Composite Coatings Deposited on Magnesium Alloy AZ31B (Mg–Al–Zn). *Electrochimica Acta,* Volume 55(2), pp. 560–571